Preprints of the 19th World Congress
The International Federation of Automatic Control
Cape Town, South Africa. August 24-29, 2014

Optimal Operating Strategy for Hybrid Railway Vehicles based on a Sensitivity Analysis

Maik Leska * **Robert Prabel** * **Harald Aschemann** * **Andreas Rauh** *

* *Chair of Mechatronics, University of Rostock, 18059 Rostock, Germany (e-mail: {Maik.Leska, Robert.Prabel, Harald.Aschemann, Andreas.Rauh}@uni-rostock.de).*

Abstract: The potential fuel savings of hybrid vehicles strongly depend on the energy management strategy, which distributes the required power between the prime mover and the additional power sources. Here, it is necessary to take into account the efficiencies of the whole propulsion system. In this paper, a novel operating strategy is developed that considers the efficiencies of all major components of the propulsion system. Fuel-optimal load points are calculated off-line by using a numerical sensitivity analysis which takes the fuel consumption as well as the variable state of charge of the energy storage system (ESS) into consideration. Using these fuel-optimal load points, the optimal operating strategy is determined by means of an optimization approach which depends on the duty cycle itself.

Keywords: Optimal operating strategy, hybrid railway vehicles, sensitivity analysis, optimization, dynamic programming

1. INTRODUCTION

Hybrid vehicles have a promising potential to reduce fuel consumption by essentially improving the energy efficiency. In this context, railway system suppliers worldwide invest in research and development of such frameworks. Generally, a hybrid power train uses more than one power source. It combines a combustion engine with a power supplement from an energy storage device. The choices of the energy storage (ESS), further system components, and the overall propulsion chain depend on the vehicle's duty cycle and on other issues such as cost effectiveness as well as maintainability. The energy savings mainly depend on the duty cycle and on the capacity and time constants of the available ESS. Hillmansen and Roberts carried out a kinematic analysis of ESS which suggests a potential of up to 35 % energy savings for commuter vehicles (Hillmansen and Roberts, 2007). The result of the research work on hybrid concepts for diesel multiple units in (Hillmansen et al., 2009) calculates a potential for the reduction of the fuel consumption of up to 25 % on a fixed route. A large number of different optimized control strategies for hybrid electric vehicles have been published in the past with the aim to minimize the fuel consumption by managing the power flows of the energy sources. In particular, they can be classified into three groups (Pisu and Rizzoni, 2007):

(1) Dynamic programming approaches (Ogawa et al., 2007), (Brahma et al., 2000)
(2) Rule-based (Dittus et al., 2011), fuzzy logic (Wang and Yang, 2006), and neural network control techniques (Moreno et al., 2006)
(3) Methods based on the conversion of the electric power into an equivalent fuel consumption (Pisu and Rizzoni, 2007).

In comparison to road-based traffic, the great advantage during the development of operating strategies for hybrid railway vehicles is the fact that the duty cycles are known beforehand. Thereby, optimal operating modes can be computed almost completely off-line as in (Leska et al., 2013). Here, a parameter optimization is used to calculate the fuel optimal operating strategy. For each acceleration and cruising phase, one optimization parameter describing the support of the ESS is introduced. This leads to a similar treatment of all load points within the same acceleration period and, furthermore, to a high number of optimization parameters.
In this paper, an optimization approach with only one optimization parameter is developed by the usage of a sensitivity analysis. In Sec. 2, the simulation structure for a basic diesel hybrid railway vehicle is summarized. Based on this simulation model, fuel-optimal load points are calculated in Sec. 3 and the optimization approach is described which aims at reducing the fuel consumption by adjusting the operating strategy. Sec. 4 concludes this paper and gives an outlook on future research.

2. MODELING OF A BASIC DIESEL PARALLEL HYBRID RAILWAY VEHICLE

The power train of a basic parallel hybrid railway vehicle mainly consists of an internal combustion engine (ICE), an energy storage device and an additional propulsion system (Leska et al., 2012). In Fig. 1, a simplified structure of the modeled diesel parallel hybrid railway vehicle is presented. Here, the ICE is supported by an electric motor/generator (M/G), which is directly connected to the drive shaft. The power for the electric motor is supplied by a Lithium Ion battery. Furthermore, the battery provides the power for the electric auxiliaries. The power transmission from the ICE and the M/G is realized via a mechanic gear box. The clutches C1 and C2 separate either the ICE and/or the M/G from the drive shaft. By this architecture, the following six operating modes are available:

- Mode 1: Pure ICE
- Mode 2: Pure M/G
- Mode 3: Boosting

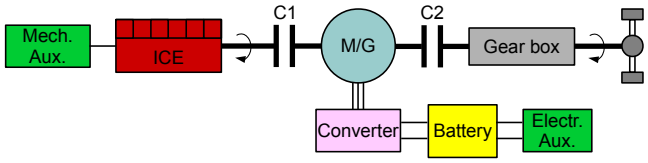

Fig. 1. Architecture of a basic diesel parallel hybrid railway vehicle.

- Mode 4: Load level increase
- Mode 5: Coasting
- Mode 6: Recuperation

In Mode 1, the ICE provides the total power demand. Mode 2 is the pure electric mode, thus, only the electric motor is active. In Mode 3, the power boost mode, both the electric motor and the ICE operate simultaneously. In the load level increase (Mode 4), the operating point of the ICE provides more power than required for following the pre-specified duty cycle. The excess power is used for recharging the ESS. This mode is also used at standstill to fully recharge the ESS. In this phase, the clutch C2 is open. In Mode 5, the coasting mode, neither the electric motor nor the combustion engine are running, while the vehicle is decoupled from all engines by opening C1 and C2. Finally, in Mode 6, the recuperation mode, kinetic energy of the vehicle is recovered in deceleration phases. The clutch C1 is opened to separate the ICE from the drive shaft. In all six operating modes, the ICE is running to supply the mechanical auxiliaries with the required power.
In Fig. 2, the simulation structure reflecting the system architecture according to Fig. 1 is given. Only the main effects contributing to the longitudinal dynamics of the power train are modeled. The individual blocks represent the component models of the hybrid system. For each component, low-order models based on dynamic equations and static characteristic maps were derived and implemented in Matlab/Simulink. The arrows represent the numerical evaluation order of the components and not the directions of power flow. Note that this evaluation order is opposed to the direction of power flow, corresponding to an inverse problem. Therefore, the inputs of the simulation approach are the velocity and altitude profiles, whereas the outputs are the load points and the fuel consumption of the ICE and the state of charge σ of the battery (Guzzella and Sciarretta, 2005). According to the control strategy, the control unit distributes the requested power for tracking the duty cycle between the ICE and the M/G. In the following section, a short description of the component models is given. The modeling of the clutches and of the converter will not be described. These elements are represented, for the sake of simplicity, by constant efficiency factors.

2.1 Vehicle

The modeling of the vehicle is based on the equation of motion

$$F_w = m_{veh} \cdot a + F_{res} + F_{inc}\,, \tag{1}$$

where F_w denotes the force at wheel, m_{veh} the mass of the vehicle, a the acceleration of the vehicle, F_{res} the resistance forces, which include the air resistance and rolling resistance, and $F_{inc} = m_{veh} \cdot g \cdot \sin(\gamma)$ the inclination force.

According to (Wende, 2003), the maximum force at wheel $F_{w,max}$ is limited by the rail wheel contact as follows

$$F_{w,max} = \mu_T\, G_T\,. \tag{2}$$

Here, G_T represents the weight of the powered set of wheels and μ_T denotes the adhesion coefficient which depends on the actual velocity v of the vehicle. The adhesion coefficient μ_T is calculated as

$$\mu_T = k_1 + \frac{k_2}{k_3 + v}$$

with the constants k_1, k_2 and k_3 by *Curtius* and *Kniffler* (Wende, 2003). The minimum force at wheel $F_{w,min}$ can be determined by

$$F_{w,min} = -\mu_B\, G_F\,, \quad F_{w.min} \le F_w \le F_{w,max}\,,$$

where G_F indicates the weight of the train and μ_B the adhesion coefficient for braking (Wende, 2003).

2.2 Axle Gear

The axle gear transmits the power from the drive shaft to the wheels. With the torque at wheel $T_w = F_w \cdot r_w$ (r_w: wheel radius) and the angular velocity of the wheels $\omega_w = v/r_w$, the torque T_{ag} and the angular velocity ω_{ag} at the input of the axle gear can be computed by

$$T_{ag} = \frac{T_w}{i_{ag} \cdot \eta_{ag}^d} \quad \text{and} \quad \omega_{ag} = \omega_w \cdot i_{ag}\,. \tag{3}$$

The efficiency η_{ag} and the gear ratio i_{ag} of the gear box are constant. The exponent d has to be chosen according to the direction of the power flow. For a positive power flow, directed from the propulsion system to the wheels, its value is $d = 1$. In the case of a negative power flow (for a power flow in opposite direction) a negative exponent $d = -1$ is used.

2.3 Mechanic Gear Box

The mechanic gear box transmits the power from the propulsion system to the axle gear; it consists of a mechanical gear set with twelve different gears $z \in \{1, \ldots, 12\}$ with fixed gear ratios $i_{gb}(z)$. Depending on the exponent d, the torque T_{gb} and the angular velocity ω_{gb} at the input of the mechanical gear set can be stated as

$$T_{gb} = \frac{T_{ag}}{\eta_{gb}^d \cdot i_{gb}(z)} \quad \text{and} \quad \omega_{gb} = \omega_{ag} \cdot i_{gb}(z)\,. \tag{4}$$

The gear z and, consequently, the gear ratio $i_{gb}(z)$ are determined in each time step. For that purpose, the shifting angular velocities

$$\omega_{up} = g_{up}\,(z, T_{ag}) \quad \text{and} \quad \omega_{down} = g_{down}\,(z, T_{ag}) \tag{5}$$

are calculated and compared with the actual angular velocity ω_{gb}. The gear will be shifted upwards if $\omega_{gb} \ge \omega_{up}$ holds; it is shifted downwards for $\omega_{gb} \le \omega_{down}$.

2.4 Internal Combustion Engine

The ICE represents the primary propulsion system. The simulation inputs are the angular velocity ω_{ICE} and the power P_{ICE} to be provided by the ICE. With their knowledge, the fuel consumption of the ICE can be computed. For all simulation and optimization stages, the specific fuel consumption map shown in Fig. 3 is used.

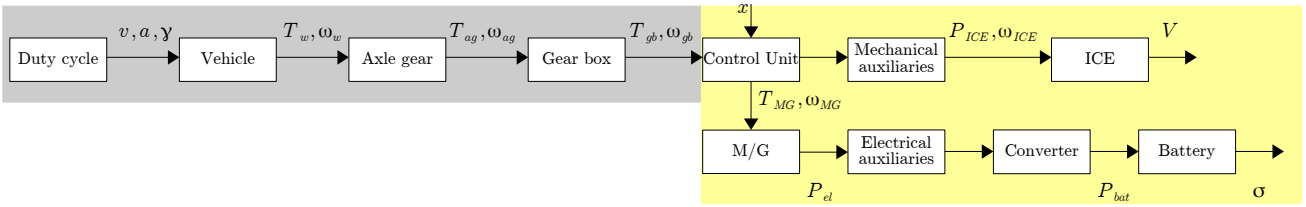

Fig. 2. Simulation structure of a diesel hybrid railway vehicle.

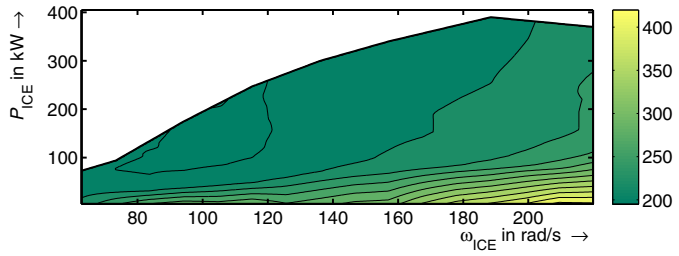

Fig. 3. Specific fuel consumption b_e in g/kWh depending on the angular velocity ω_{ICE} and the power P_{ICE}.

Using a linear 2D-interpolation, the specific fuel consumption b_e can be determined and, thereby, the absolute fuel consumption for the ICE becomes

$$V(t) = \int_0^t \frac{P_{ICE}(\tau) \cdot b_e(\tau)}{\rho_{fuel}} d\tau . \tag{6}$$

2.5 Electric Motor/Generator

The electric motor/generator (M/G) unit is used to support the ICE during traction phases, to convert mechanical energy into electrical energy and, finally, to charge the energy storage device during braking phases.

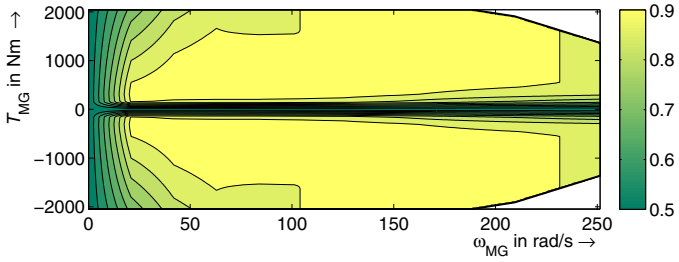

Fig. 4. Efficiency η_{MG} of the M/G depending on the rotational speed ω_{MG} and the torque T_{MG}.

By multiplication of the simulation block inputs T_{MG} and ω_{MG}, the mechanical power $P_{MG} = T_{MG} \cdot \omega_{MG}$ can be obtained. Depending on the direction of the power flow ($d = 1$: positive power flow; $d = -1$: negative power flow), the electric power P_{el} can be computed as $P_{el} = \frac{P_{MG}}{\eta_{MG}^d}$.

The efficiency η_{MG} is determined by a linear 2D-interpolation in the efficiency map of the electric motor/generator, see Fig. 4, with ω_{MG} and T_{MG} as inputs.

2.6 Energy Storage

A Lithium Ion battery consisting of $n_{par} = 9$ branches in electric parallel connection, each branch itself contains $n_{ser} = 192$ cells in series connection, is used as energy storage device. In traction phases, it provides power to the electric motor and in braking phases it stores the recuperated energy. The simplified model of the battery is derived at cell level on the basis of (Rauh and Aschemann, 2012) for the equivalent electrical circuit of the battery illustrated in Fig. 5. It consists of a state-of-charge-controlled voltage source U_{oc} in series with a constant resistance R_{ser}, representing Ohmic losses.

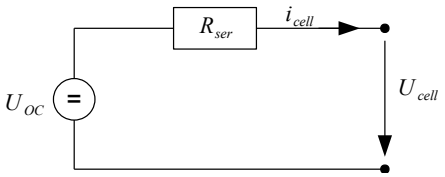

Fig. 5. Equivalent electrical circuit for the battery.

The terminal voltage U_{cell} of the cell is defined by the cell current

$$i_{cell} = \frac{P_{el}}{n_{par} \cdot n_{ser}} \cdot \frac{1}{U_{cell}} . \tag{7}$$

according to

$$U_{cell} = U_{oc} - R_{ser} \cdot i_{cell} . \tag{8}$$

Using equations (8) and (7), the output variables U_{bat} and i_{bat} can be formulated as

$$U_{bat} = U_{cell} \cdot n_{ser} \quad \text{and} \quad i_{bat} = i_{cell} \cdot n_{par} . \tag{9}$$

The state of charge σ results from the cell current i_{cell}, its initial value $\sigma_{init} = \sigma(0)$, and the nominal capacity C_{nom} of one cell

$$\sigma(t) = \sigma(0) - \int_0^t \frac{i_{cell}(\tau)}{C_{nom}} d\tau . \tag{10}$$

3. OPTIMIZATION OF THE FUEL CONSUMPTION BY ADJUSTING THE OPERATING STRATEGY

An operating strategy for a hybrid vehicle mainly means to allocate the demanded traction power among the propulsion systems (ICE and M/G). For that purpose, the boost ratio x is introduced which allows for splitting the required traction power $P_{gb} = T_{gb} \cdot \omega_{gb}$ between the ICE and the M/G. In Mode 1, the power values of the ICE and the M/G are defined as

$$P_{ICE} = (1 - x) \cdot P_{gb}, \quad P_{MG} = x \cdot P_{gb} . \tag{11}$$

If Mode 4 (load level increase) becomes active, the power of the ICE and the M/G are calculated by

$$P_{ICE} = -x \cdot (P_{max} - P_{gb}) + P_{gb}, \quad P_{MG} = P_{gb} - P_{ICE} , \tag{12}$$

where P_{max} denotes the maximum recuperation power which is limited by the maximum ICE power and the maximum power of the ESS.

The optimization is done in two steps. First, the optimal boost ratio x in Mode 1 and 4 is computed by a sensitivity analysis. Based on these results, a bisection method is used in the following step to calculate the fuel optimal operating strategy for the trajectory depicted in Fig. 6. In the upper plot a typical velocity profile for a regional train, e.g. in the low mountain range of Germany, is shown with the corresponding inclination profile presented in the lower plot.

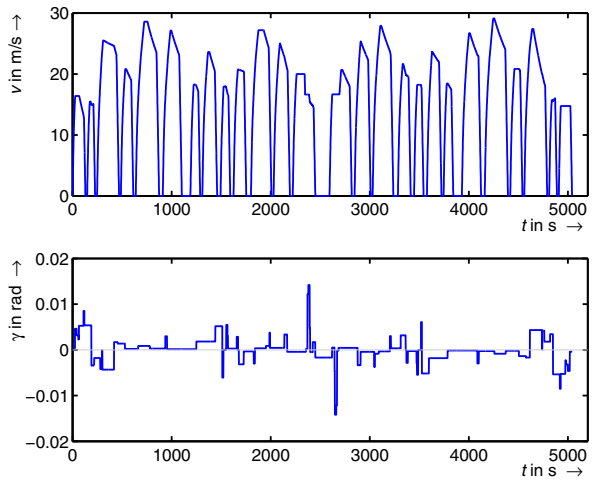

Fig. 6. Reference trajectory.

The considered vehicle is a two-coach diesel multiple unit (DMU), $VT642$, with one propulsion unit (consisting of an ICE, a gear box, a M/G and a battery) per coach and an increased vehicle mass by 4000 kg accounting for the additional system components of a hybrid system architecture, such as the electric motor and the ESS. The auxiliaries are characterized by a constant power demand, half of which has to be provided by the ICE and half by the ESS. As a result, the ICE is operated permanently during the whole operating time. To allow for a comparison of the achievable fuel savings of the hybrid railway vehicle, a simulation with a classical diesel vehicle is performed. The resulting fuel consumption is employed as a reference V_{ref} for the following optimization results with the hybrid vehicle.

3.1 Evaluation of the optimal boost ratio x in Mode 1

To evaluate the optimal boost ratio x, a numerical sensitivity analysis is performed by running the yellow shaded part of the simulation structure in Fig. 2 in different load points $(\omega_{gb}^i, T_{gb}^j)$. For each of them $k \in \{1,..,100\}$ simulations are performed with an initial state of charge of $\sigma_{init} = 0.5$ and a simulation time of 30 s, but varying boost values $x_k^{i,j} \in [0,1]$. Corresponding to the resulting fuel consumption $V_k^{i,j}$ and the resulting state of charge $\sigma_k^{i,j}$, the optimal boost ratio $x^{i,j}$ for each load point $(\omega_{gb}^i, T_{gb}^j)$ can be determined by the evaluation of the optimal boost sensitivity $s_b^{i,j}$. It indicates the potential fuel savings by discharging the ESS by one percent of its the nominal capacity and can be calculated by the resulting fuel consumption $V_k^{i,j}$, state of charge $\sigma_k^{i,j}$ and the reference values $V_d^{i,j}$ and $\sigma_d^{i,j}$ of a pure diesel propulsion $(x_k^{i,j} = 0)$ as

$$s_b^{i,j} = \max_{x_k^{i,j}} \left\{ \frac{V_d^{i,j} - V_k^{i,j}}{\sigma_d^{i,j} - \sigma_k^{i,j}} \right\} \cdot 100\,. \tag{13}$$

The higher the boost sensitivity $s_b^{i,j}$, the more efficient is a support of the diesel engine by the electric motor at the current load point $(\omega_{gb}^i, T_{gb}^j)$.

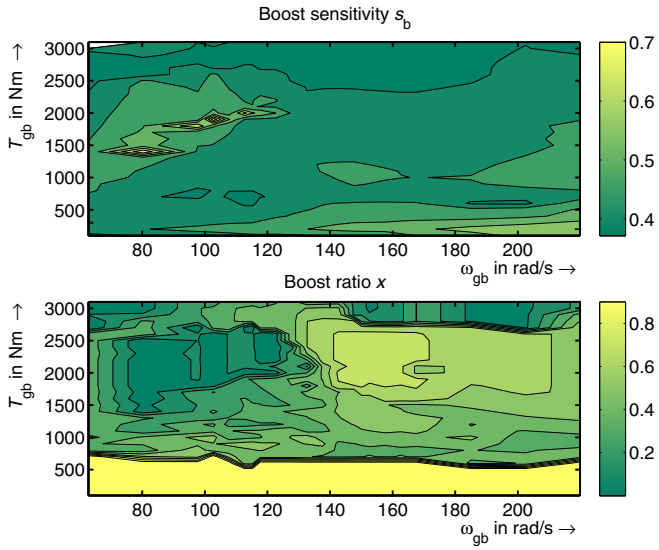

Fig. 7. Optimal boost sensitivities s_b and corresponding values of the boost x.

Fig. 7 shows the best specific fuel savings for the different load points and the corresponding boost values x. In the upper plot, the optimal boost sensitivities s_b are shown; the larger s_b, the higher are the fuel savings. The highest boost sensitivities of $s_b = 0.7$ are possible at low speeds and medium loads, but there exists only a few load points with such high benefits. In average, boost sensitivities of $s_b = 0.45$ are possible. In the lower plot of Fig. 7, the corresponding values of the boost ratio x are visualized. At low torques T_{gb}, a pure electric drive $(x = 1)$ is the most effective way; in all other load points, the optimal boosting factor changes nearly from point to point.

3.2 Evaluation of the optimal boost ratio x in Mode 4

A further sensitivity analysis is done to compute the best boost ratio $x \in [-1,0]$ during the load level increase (Mode 4). Again, $k \in \{1,..,100\}$ simulations are performed for different load points $(\omega_{gb}^i, T_{gb}^j)$, 30 s simulation time and varying boost values $x_k^{i,j} \in [-1,0]$, but the initial state of charge is now chosen as $\sigma_{init} = 0.4$. Corresponding to the resulting fuel consumption $V_k^{i,j}$ and the resulting state of charge $\sigma_k^{i,j}$, the optimal boost ratio $x^{i,j}$ for each load point $(\omega_{gb}^i, T_{gb}^j)$ can be determined by the evaluation of the optimal load increase sensitivity $s_l^{i,j}$. It indicates the additional fuel consumption for charging the battery by one percent of its nominal capacity. It can be calculated with the reference values $V_d^{i,j}$, $\sigma_d^{i,j}$ of a pure diesel propulsion $(x_k^{i,j} = 0)$ according to

$$s_l^{i,j} = \min_{x_k^{i,j}} \left\{ \frac{V_k^{i,j} - V_d^{i,j}}{\sigma_k^{i,j} - \sigma_d^{i,j}} \right\} \cdot 100\,. \tag{14}$$

The lower the load increase sensitivity $s_l^{i,j}$, the more efficient is the load increase mode at the current load point $(\omega_{gb}^i, T_{gb}^j)$.

Fig. 8 presents the optimal load increase sensitivities s_l in the upper plot and the corresponding values of the boost x as a result of a load level increase in the lower plot. The lowest values of the load increase sensitivity s_l are located at low speeds and low loads. Here, only 0.5 l are needed to recharge the ESS by one percent of its energy content. In average, 0.55 l are necessary to recharge the ESS by one percent.

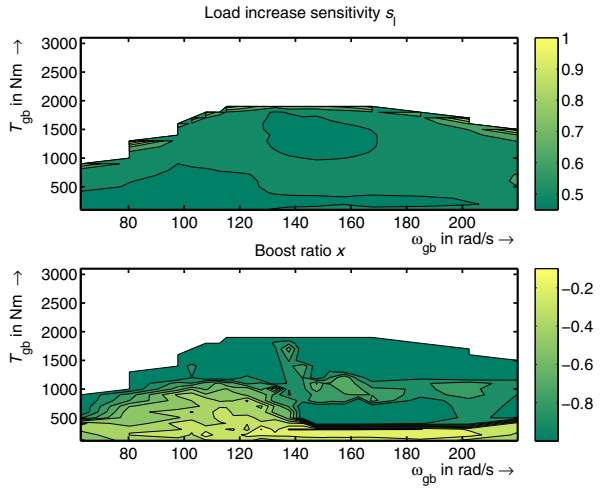

Fig. 8. Optimal load increase sensitivities s_l and corresponding values of the boost ratio x.

3.3 Calculation of a fuel optimal operation strategy using the bisection method

Basically, the maximum support of the ICE by the electric motor ($x = 1$) leads to the maximum absolute fuel savings, but causes also a higher decrease of the state of charge σ. Such an operating strategy usually results in a smaller state of charge σ at the final destination than at the beginning, or in the worst case to a completely discharged ESS. The operating costs are then composed of the costs for the used fuel and the costs for recharging the ESS to its initial state of charge σ_{init}. Due to this fact and for a fair comparison w.r.t. the fuel consumptions between a purely diesel driven and a hybridized vehicle, an identical battery charge at the starting point $\sigma(0) = \sigma_{init}$ and the final destination $\sigma(t_f)$ is demanded in the following. This implies that only the recuperated energy should be used to support the ICE during traction phases. Hence, the boosting mode is only used at load points with the highest efficiencies according to the results of the sensitivity analysis. To guarantee a balanced battery charge for the duty cycle, the parameter s_{lim} is introduced which defines the minimum value of s_b as shown in Fig. 9. At load points with a lower value of s_b than the minimum value s_{lim}, the boosting mode is avoided.

A load level increase is only meaningful if the resulting additional fuel consumption is smaller than the fuel savings which can be achieved by the boosting mode using the increased energy content of the ESS. This is only the case if there exist load points with a lower value of s_l than the value of s_{lim}. For the chosen scenario, such load points do not exist, hence, Mode 4 is neglected.

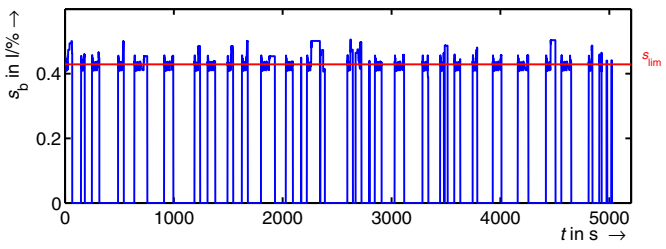

Fig. 9. Boost sensitivities s_b for the given duty cycle.

The fuel optimal operating strategy is calculated by a bisection method, which adjusts the optimization parameter s_{lim} until the state of charge σ is balanced for the given duty cycle $\sigma(0) = \sigma(t_f)$. In every iteration step, one simulation run of the complete model shown in Fig. 2 is performed for a certain factor s_{lim}. The resulting fuel consumption V of the hybrid vehicle is 19.9 % less than V_{ref} of the standard diesel vehicle. Fig. 10 shows the corresponding development of the state of charge σ, which is identical at the starting point and at final destination $\sigma(0) = \sigma(t_f) = 0.5$.

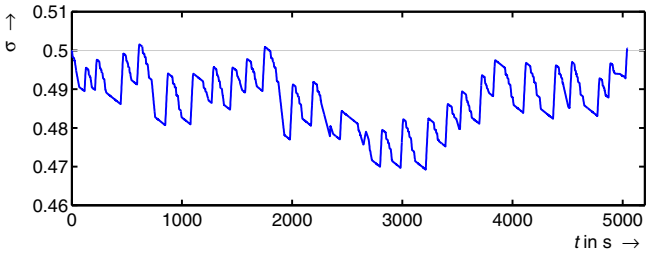

Fig. 10. Progression of the state of charge σ during the duty cycle for the sensitivity-based optimization approach.

3.4 Global fuel optimal operating strategy

For a comparison with the sensitivity-based optimization approach, the global fuel optimal operating strategy is determined by means of the dynamic programming technique of Bellman (DP). This approach is a computationally expensive algorithm calculating the optimal control sequence for each time step. The algorithm finds the optimal control sequence on a chosen grid in negative time direction based on Bellman's optimality principle: "Regardless of the decisions taken to enter a particular state in a particular stage, the remaining decisions made for leaving that stage must constitute an optimal policy" (Bellman, 1952). The resulting operating strategy is characterized by frequent switches in the boosting factor x, but the results can be regarded as the global optimum. In general, the dynamic programming is used to calculate the optimal control sequence for multi-stage decision processes.

First, the optimization problem is discretized into $k \in \{0,...,N\}$ with $N = 5043$ time steps which means a step length of $\Delta t = 1$ s, in $i \in \{1,...I\}$ with $I = 2001$ values for the state of charge $\sigma^i(k) \in [0.4, 0.6]$ and in $j \in \{1,...,M\}$ with $M = 21$ values for the boost ratio $x^j(k) \in [-1, 1]$. The resulting state of charge

$$\sigma(k+1) = f(\sigma^i(k), x^j(k)) \tag{15}$$

and the actual costs (fuel consumption)

$$V_0(k) = g(\sigma^i(k), x^j(k)) \tag{16}$$

are computed then in each decision k by running either the lower path of the yellow shaded part of the simulation model given in Fig. 2 or the upper path. Hence, the minimum costs $V^{N-(k+1)}$ for the remaining trajectory can be obtained for all states $\sigma^i(k)$ by solving the following optimization problem

$$V^{N-k}(\sigma^i(k)) = \min_{x^j(k)}\{V_0(\sigma^i(k), x^j(k)) + V^{N-(k+1)}(\sigma^i(k-1))\}, \tag{17}$$

where $V^{N-(k+1)}(\sigma^i(k-1))$ denotes the remaining costs starting from the resulting state $\sigma(k+1)$ up to the final stage N.

The dynamic programming starts at the stage $k = N-1$ and is evaluated according to Bellman's optimality principle in negative time direction until the first stage $k = 0$ is reached. For that purpose, at first, the load points $(T_{gb}(k), \omega_{gb}(k))$ that are needed as simulation inputs are identified off-line for every time step k by evaluating the grey shaded part of the simulation model in Fig. 2. With the load point $(T_{gb}(k), \omega_{gb}(k))$ and the initial state of charge $\sigma^i(k)$, the resulting state of charge $\sigma(k+1)$ and the actual costs $V_0(k)$ can be computed. If the resulting state of charge $\sigma(k+1)$ is not equal to one of the N discrete values of the state of charge σ^i, the remaining costs $V^{N-(k+1)}$ will be determined by an interpolation between the two closest states to the resulting states $\sigma(k+1)$. The overall costs then can be calculated by

$$V^N(x(0)) = \sum_{k=0}^{N-1} (V_0(\sigma(k), x(k)) + V(x(N))). \tag{18}$$

For the given scenario in this paper, the resulting fuel consumption obtained by dynamic programming is 20.2 % smaller than the reference fuel consumption V_{ref} of the standard diesel vehicle. The corresponding progression of the state of charge σ of the battery is given in Fig. 11.

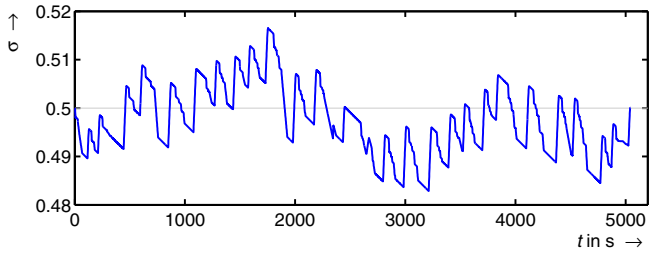

Fig. 11. Progression of the state of charge σ during the duty cycle for the dynamic programming approach.

4. CONCLUSIONS

In this paper, a new operating strategy is developed for hybrid railway vehicles. The power split between the diesel engine and the electric motor occurs only in optimal load points which are calculated off-line beforehand by a sensitivity analysis. For that purpose, a simulation model is developed containing the main effects contributing to the longitudinal dynamics of the main components of the power train. The adjustment of the operating strategy to the driving cycle can be performed by only one parameter s_{lim}, which has to be chosen in such a way that the battery charge at the starting point and at final destination is balanced. The performance of the new operating strategy is nearly identical to the globally optimal solution obtained by the dynamic programming. Due to the fact that only one parameter is necessary to adapt the operating strategy to the driving cycle, the presented approach is also very promising for an on-line power management. For that, an adaptive and/or a model predictive controller shall be developed in future work.

REFERENCES

Bellman, R. (1952). On the theory of dynamic programming. In *Proceedings of the national Academy of Sciences, USA*.

Brahma, A., Guezennec, Y., and Rizzoni, G. (2000). Optimal energy management in series hybrid electric vehicles. In *Proceedings of the American Control Conference, Chicago*, pp. 60–64.

Dittus, H., Hülsebusch, D., and Ungethüm, J. (2011). Reducing dmu fuel consumption by means of hybrid energy storage. *European Transport Research Review, Springer-Verlag*, vol. 3(3), pp. 149–159.

Guzzella, L. and Sciarretta, A. (2005). *Vehicle propulsion systems: introduction to modeling and optimization*. Springer, Berlin; New York.

Hillmansen, S. and Roberts, C. (2007). Energy storage devices in hybrid railway vehicles: a kinematic analysis. *Proceedings of the Institution of Mechanical Engineers, Part D: Journal of Automobile Engineering*, vol. 221(1), pp. 135–140.

Hillmansen, S., Roberts, C., and McGordon, A. (2009). Final report: Hybrid concept evaluation. URL `www.birmingham.ac.uk/Documents/college-eps/railway/HybridRailReportDMUV1.pdf`.

Leska, M., Grüning, T., Aschemann, H., and Rauh, A. (2012). Optimization of the longitudinal dynamics of parallel hybrid railway vehicles. In *IEEE International Conference on Control Applications (CCA), Dubrovnik*, pp. 202–207.

Leska, M., Grüning, T., Aschemann, H., and Rauh, A. (2013). Optimal trajectory planning for standard and hybrid railway vehicles with a hydro-mechanic transmission. *In European Control Conference ECC13, Zurich, Switzerland*.

Moreno, J., Ortuzar, M., and Dixon, J. (2006). Energy-management system for a hybrid electric vehicle, using ultracapacitors and neural networks. *IEEE Transactions on Industrial Electronics*, vol. 53(2), pp. 614–623.

Ogawa, T., Yoshihara, H., Wakao, S., Kondo, K., and Kondo, M. (2007). Energy consumption analysis of fc-edlc hybrid railway vehicle by dynamic programming. In *European Conference on Power Electronics and Applications, Aalborg*, pp. 1–8.

Pisu, P. and Rizzoni, G. (2007). A comparative study of supervisory control strategies for hybrid electric vehicles. *IEEE Transactions on Control Systems Technology*, vol. 15(3), pp. 506–518.

Rauh, A. and Aschemann, H. (2012). Sensitivity-based state and parameter estimation for lithium-ion battery systems. In *IX. Intl. Conference System Identification and Control Problems, SICPRO'12, Moscow, Russia*.

Wang, A. and Yang, W. (2006). Design of energy management strategy in hybrid vehicles by evolutionary fuzzy system part i: Fuzzy logic controller development. In *The Sixth World Congress on Intelligent Control and Automation (WCICA)*.

Wende, D. (2003). *Fahrdynamik des Schienenverkehrs (in German)*. Vieweg+teubner Verlag.